Research article

Internet-based remote assembly of micro-electro-mechanical systems (MEMS)

Yantao Shen
Ning Xi
King W.C. Lai and
Wen J. Li

The authors

Yantao Shen and **Ning Xi** are based at Department of Electrical and Computer Engineering, Michigan State University, Michigan, USA.
King W.C. Lai and **Wen J. Li** are based at Center for Micro and Nano Systems, The Chinese University of Hong Kong, Hong Kong SAR, China.

Keywords

Assembly, Internet, Microsensors, Manufacturing systems

Abstract

This paper presents our development of a novel Internet-based E-manufacturing system to advance applications in micromanipulation and microassembly using an *in situ* polyvinylidene fluoride (PVDF) piezoelectric sensor. In this system, to allow close monitoring of magnitude and direction of microforces (adhesion, surface tension, friction, and assembly forces) acting on microdevices during assembly, the PVDF polymer films are used to fabricate the highly sensitive 1D and 2D sensors, which can detect the real-time microforce and force rate information during assembly processes. This technology has been successfully used to perform a tele-assembly of the surface MEMS structures with force/visual feedback via Internet between USA and Hong Kong. Ultimately, this E-manufacture system will provide a critical and major step towards the development of automated micromanufacturing processes for batch assembly of microdevices.

Electronic access

The Emerald Research Register for this journal is available at
www.emeraldinsight.com/researchregister

The current issue and full text archive of this journal is available at
www.emeraldinsight.com/0144-5154.htm

Assembly Automation
Volume 24 · Number 3 · 2004 · pp. 289–296
© Emerald Group Publishing Limited · ISSN 0144-5154
DOI 10.1108/01445150410549782

1. Introduction

Microfabrication methods such as bulk-micromachining and surface-micromachining are commonly used to make devices for a wide variety of applications, including sensing, optical and wireless communications, digital display, and biotechnology. Despite the enormous research in creating new applications with MEMS, the research efforts at the backend, such as automatic microassembly and packaging, are relatively limited. One main reason for such limitation is that the manipulation of microsized objects is poorly understood (Nelson *et al.*, 1998). Owing to scaling effects, unmodeled forces that are insignificant at the macroscale become dominant at the microscale (Fearing, 1995). For example, when the part is less than 1 mm in size, adhesive forces between the manipulator and the part can be significant compared to gravitational forces. These adhesive forces arise primarily from surface tension, van der Waals, and electrostatic attractions and the measurement of those forces will be a critical factor for micropart manipulation. As a case in point, manufacturing processes which are capable of efficiently assembling MEMS devices such a micromirror in optical switches have not been developed, partially because, at the microscale, structures are fragile and easily breakable. They typically break at the micronewton force range that cannot be reliably measured by the existing force sensors (Fung *et al.*, 2002). The micromirror components are usually surface optomechanical structures. They lie on the surface of substrate after fabrication processes, as shown in Figure 1(a). An assembly process is needed to rotate it up to a perpendicular position as shown in Figure 1(b) and (c). Currently, the most straightforward and flexible method is to use microprobes to physically manipulate the mirror into position. However, this process can be inherently risky without the knowledge of the force(s) being applied and slow without some level of precision and automation. It has been widely realized that there have not been a reliable sensor for accurately obtaining microforce data during assembly, and assembly method for effectively feeding back the microcontact force/impact in the micromanipulation (Böhringer *et al.*, 1999; Carrozza *et al.*, 2000; Cohn *et al.*, 1998; Koelemijer *et al.*, 1999; Yamagata and Higuchi, 1995; Zesch and Fearing, 1998). As a result, the microdevices are often damaged during assembly,

This work is supported in part by the NSF Grants IIS-9796300, IIS-9796287, EIA-9911077, Hong Kong Research Grants Council (CUHK4206/00E), and by the Chinese Academy of Sciences' Distinguished Overseas Scholar Grant.

Figure 1 (a) Microscope image of micromirrors on the chip; (b) the force is applied at the mirror; and (c) an automatic latches lock the mirror in upright position

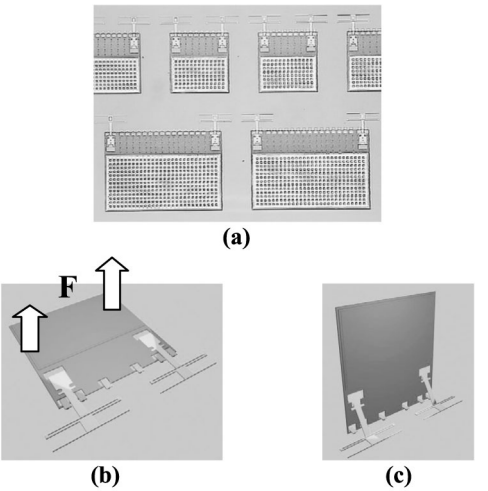

which decrease the overall yield and drives up cost significantly. It has been estimated that assembly cost of microdevices can run as high as 80 percent of the total production cost (Kenny, 2001).

The objective of this project is to develop a feasible and versatile solution in microassembly and micromanufacture, i.e. designing a highly sensitive polyvinylidene fluoride (PVDF) force sensor to measure microcontact/impact force and its rate so as to enable a feedback of microforce during the micromanufacture process. By integrating the developed PVDF sensory system on a micromanipulator, the microforce can be efficiently fed back and thus, keep a safety margin during assembly and manufacture. Furthermore, on the basis of the above work, an Internet-based remote assembly (micro E-manufacturing) system with force/visual feedback was built successfully for tele-assembly of microdevices. Its applications could be an important step to make reliable and high yield batch fabrication, assembly of MEMS.

This paper is organized as follows. Section 2 reviews the novel microforce sensor and its processing unit. System integration is described in Section 3. Section 4 proposes an Internet-based remote assembly (micro E-manufacturing) system for surface MEMS devices and gives some experimental results on tele-microassembly of the micromirrors. Finally, we conclude the work in Section 5.

2. Sensor modeling and design

2.1 PVDF microforce/force rate sensors

As shown in Figure 2, for the 1D sensor model, the relationship between the output voltage $V(t)$ and the microcontact force rate $\dot{F}(t)$ can be obtained as (Benech *et al.*, 1996; IEEE Standard, 1987; Measurement Specialties Inc., 1999):

$$V(t) + \lambda \dot{V}(t) = B\dot{F}(t) \tag{1}$$

where

$$\lambda = R_P C_P \quad \text{and} \quad B = \frac{R_P W L d_{31} h\left(L_0 + \frac{L}{2}\right)}{2I}$$

are constants. R_P and C_P are the resistance and capacitance of the PVDF film, respectively. d_{31} is the transverse piezoelectric coefficient. I represents the inertial moment of cross-sectional area a. The neutral axis of the film beam is assumed to pass through the centroid of the cross-sectional area a.

Based on the 1D model, as shown in Figure 3, the 2D sensor was designed using a parallel beam structure. In each direction, a two-piece parallel beam is used to improve the rigidity of the structure and, at the same time, to keep the sensitivity of the force sensing in that direction. It can also be seen that this structure provides

Figure 2 Illustration of 1D sensor structure

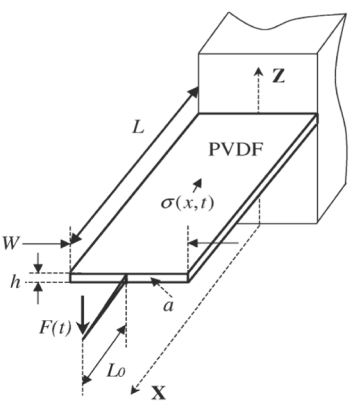

Figure 3 Illustration of 2D sensor structure

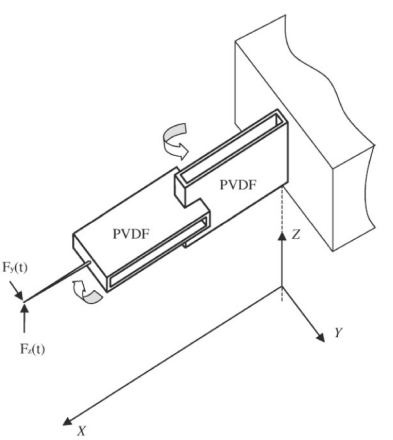

a decoupling force measurement in the Y and Z directions.

The decoupled output voltages and force rates can be represented as

$$V_Z(t) + \lambda_Z \dot{V}_Z(t) = B_Z \dot{F}_Z(t)$$
$$V_Y(t) + \lambda_Y \dot{V}_Y(t) = B_Y \dot{F}_Y(t) \quad (2)$$

2.2 Signal conditioning circuit

Preprocessing of sensed data by the circuit is critical for two reasons:

(1) to remove noises (from vibrations, temperature change, external electronic coupling noises, etc.); and
(2) to amplify and extract the desired signal which is in this case the force and force rate.

The simplified diagram of developed circuit is shown in Figure 4.

In this circuit, a differential charge amplifier was designed for the PVDF force sensor. The differential charge amplifier is based on the chopper stabilized operational amplifier TC7650C with a high input impedance $10^{12}\,\Omega$ and low bias current 1.5 pA. A high input impedance can avoid the leakage of the charge on the feedback capacitor C_{f1} and C_{f2} ($C_{f1} = C_{f2}$), and low bias current prevents the feedback capacitor from charging and discharging at excessive rates. Following the charge amplifier, a differential-to-single-ended amplifier is added. In this design, the total differential topology can reduce the common mode noises more effectively. Otherwise, by choosing the charge amplifier, the cable capacitor C_c is removed from the dynamic model of the circuit, so that a long cable can be used to connect the sensor and circuit without affecting the system performance. With the use of the charge amplifier, the sensor can measure force at a very low frequency, this is because the low corner frequency is now expanded to $f_1 = 1/2\pi R_{fi} C_{fi}$, where i represents 1 or 2.

As shown in the diagram of the circuit, resistors R_{c1} and R_{c2} ($R_{c1} = R_{c2}$) can provide electrostatic discharge (ESD) protection.

Since the vibration and thermal noises are the major high frequency disturbances of sensor signal, to reject the high frequency noises, an active low pass filter with the suitable cut-off frequency was used before the voltage output. An integrator unit in the circuit can also achieve the integration of the output voltage by time.

By considering the sensor model and the whole circuit, the global transfer function of the sensor system is

$$\frac{V_{out}(s)}{F(s)} = \frac{V_c(s) B K_c}{\lambda} \frac{\lambda s}{(1+\lambda s)(1+\tau_1 s)} \quad (3)$$

The function is a bandpass type filter. K_c is the gain of the differential-to-single-ended amplifier. τ_1 is the small time constant of the active low pass filter. Based on equation (3), by filtering this signal over an appropriate passband and then integrating it with respect to time, the microforce is achieved over this passband. In addition, the microforce rate can also be obtained without integrating the above equation by time.

2.3 Calibration and force sensing experiments

Referring to the basic physical models of the 1D and 2D PVDF sensors, Figure 5 shows the prototypes of the PVDF sensors used in the calibration and experiments. As shown in the figure, the PVDF film (1D) has the following dimensions and parameters:

Figure 4 Schematics of the developed electronic circuit

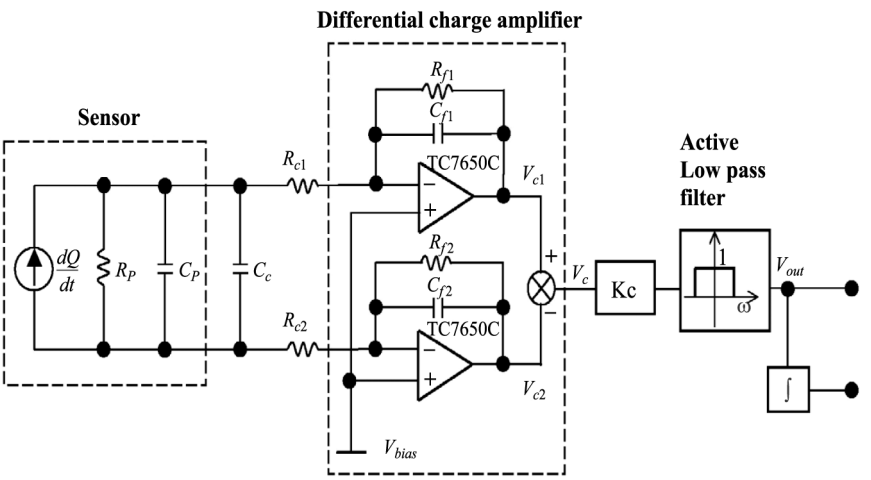

Figure 5 Prototypes of (a) 1D, and (b) 2D sensors

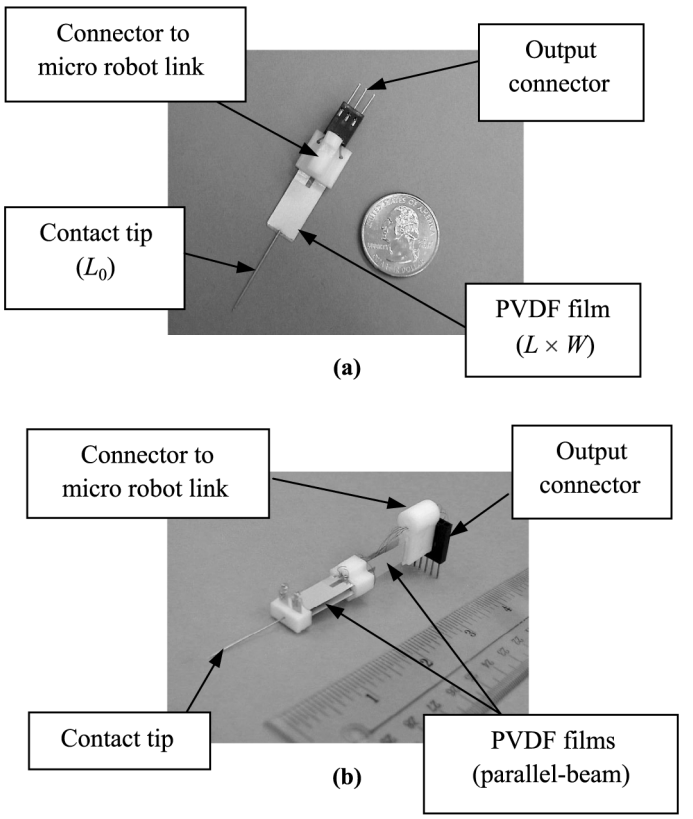

Figure 6 Comparison of theoretical and calibrated forces

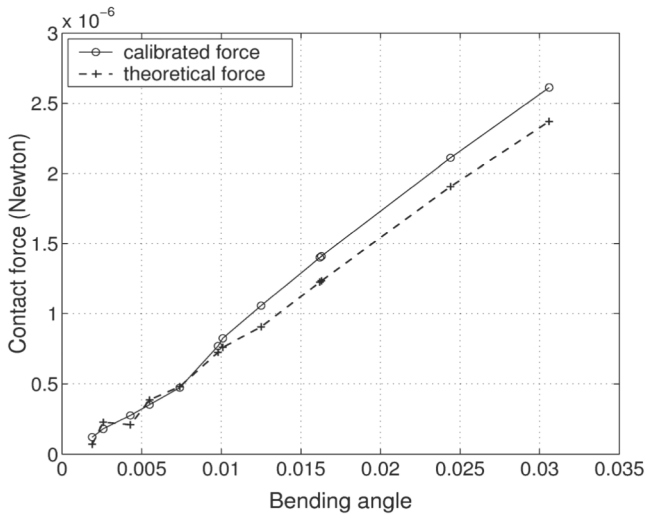

$$L_0 = 0.0225\,\text{m}, \quad L = 0.0192\,\text{m},$$

$$W = 0.0102\,\text{m}, \quad h = 28\,\mu\text{m} \quad \text{(PVDF film)},$$

$$R_\text{P} = 1.93 \times 10^{12}\,\Omega, \quad C_\text{P} = 0.90 \times 10^{-9}\,\text{F},$$

$$E = 2 \times 10^{-9}\,\text{Nm}^{-2}, \quad d_{31} = 23 \times 10^{-12}\,\text{CN}^{-1}.$$

By virtue of a precisely calibrated Mitutoyo 100x microscope (with a 50x objective and a 2x zoom), and a Sony CCD camera system, the set-up for calibration was built. The total resolution of the setup approaches 0.2106 μm/pixels in X and 0.2666 μm/pixels in Y on the image plane, so the tiny bending angle $\theta(t)$ or deflection $\delta(t)$ of the sensor beam under the microscope can be measured when a microforce is exerted.

Note that, to obtain an accurate $\theta(t)$ or $\delta(t)$ from the captured image, image processing techniques and least square method were adopted to find an optimal solution on $\theta(t)$ or $\delta(t)$. Meanwhile, based on the model equation (3), the output voltage signals transferred by the built circuit can be used to calculate the theoretical value of microcontact force. Figure 6 shows the quasi-static calibration results when a nonmagnetic, insulating and rigid block on 3-DOF platform contacted the 1D force sensor. The two curves are rather close, which clearly indicates the effectiveness of the developed sensor models.

By preliminary calibrations, the sensitivity of the 1D sensor is estimated to be 4.6602 V/μN, the 2D sensor is 2.3985 V/μN (the gap distance of two parallel PVDF films is zero). The resolutions of the sensors are both in the range of micronewton. As an important aspect of the sensor, dynamic range is an ability to respond to signals having both large and small amplitude variation. The output width of sensor system is 12 V with a quantization resolution of 0.73 mV; therefore, the output dynamic range of two sensors is 84.32 dB. In analogy with output dynamic range, the input dynamic range is thus given by the ratio of input width to the input resolution. By calibration, when the sensor tip deflects to approach 90°, the input dynamic range of the 1D sensor is estimated more than 104.4 dB; the 2D sensor is about 121.9 dB.

Furthermore, an experiment on the contact sensing was conducted. By using the 2D sensor, a continual contact-stop sensing experiment was implemented when the sensor tip acted on a planar glass surface that was setup in the ZX plane (referring to Figure 3). The 2D force signals recorded were plotted in Figure 7. The results verified the performance of sensing and self-decoupling of the 2D force sensor.

3. System integration

The piezoelectric force sensor system was integrated with a micromanipulator in the Robotics and Automation Laboratory at Michigan State University. The integrated microrobotic system, as shown in Figure 8, was used for the micromanufacture and microassembly work.

Figure 7 Response of 2D sensor when the force is exerting along *Y*

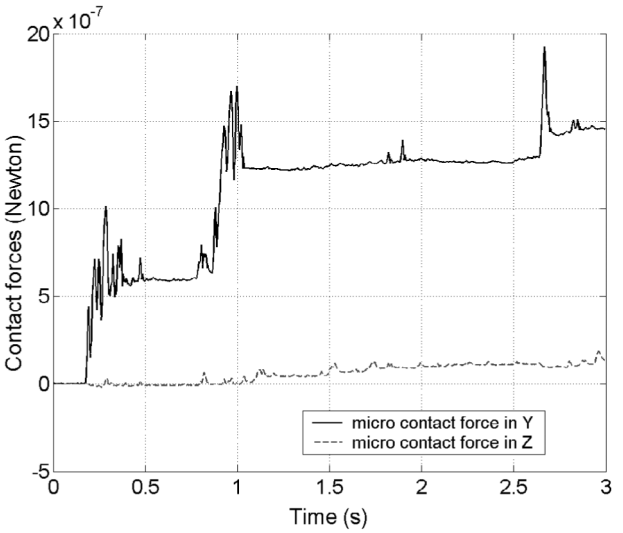

Figure 8 Integrated microrobotic system at MSU

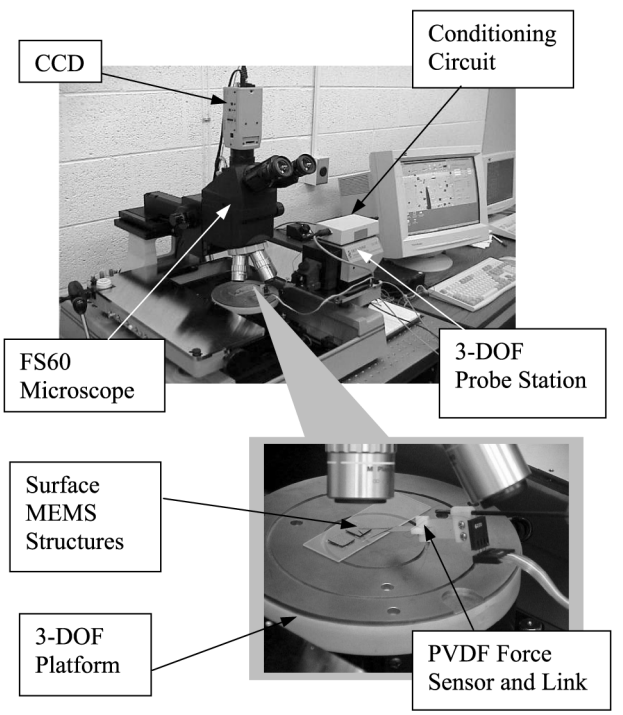

It consists of a 3-DOF micromanipulator (SIGNATONE Computer Aided Probe Station), a 3-DOF platform, a Mitutoyo FS60 optical microscope and a Sony SSC-DC50A CCD Color Video Camera. The micromanipulator is controlled by a PC-based control system. The system is an open platform, which can be connected easily with external input system such as joystick. Several motion control software and user interface have been developed using C++. They provide a flexible and user-friendly interface to interact with the external input system and operator. The 3D platform can convey the microdevices for manufacturing in time. The Mitutoyo FS60 optical microscope and a Sony SSC-DC50A CCD Color Video Camera can real-time capture the micromanufacture process and give a feed back to the visual information.

When the PVDF sensor detects the microforce, the output voltage signals from the electronic circuit could be collected via a multifunction analog/digital input/output board (AX5411H) into a PC. Then there exists a force data communication between the PC and microrobotic system. The sampling frequency of the AX5411H is 1 kHz in the experiments.

To reduce vibrations, an active vibration isolated table was used during the experimental work.

4. Tele-microassembly system

Based on the integrated system, a "micro E-manufacturing" concept is induced when we tele-assembled surface MEMS structures via Internet. In this application, a master device with force/haptic feedback is driven to teleoperate a micromanipulator with the microforce sensor to assemble MEMS devices. Based on this concept, a micromanipulator-joystick tele-microassembly platform was built at Michigan State University, as shown in Figure 9. In this platform, we can teleassmeble the MEMS devices such as micromirrors with our hands via Internet. During the assembly, not only the visual feedback is provided for observing the situations of operation, but also the use of force feedback from the microforce sensor, which can provide the human operator with the similar haptic feeling even if the operator is not in direct assembling the micromirrors. The method used in this teleoperation is the Motion-Force Transmission, in this case, the 3D movement of the joystick is sent to the 3D micromanipulator, and the microforces felt by the PVDF force sensor at the front end of micromanipulator are fed back to the joystick. By appropriately choosing the scaling laws, both microforce and movement are effectively scaled up and down between the joystick and micromanipulator. To improve the synchronization of the developed tele-microassembly system with visual/haptic feedback, the event-based methods are employed to ensure an acceptable level of synchronization of visual and haptic/force

Figure 9 E-manufacturing of micromirrors and system

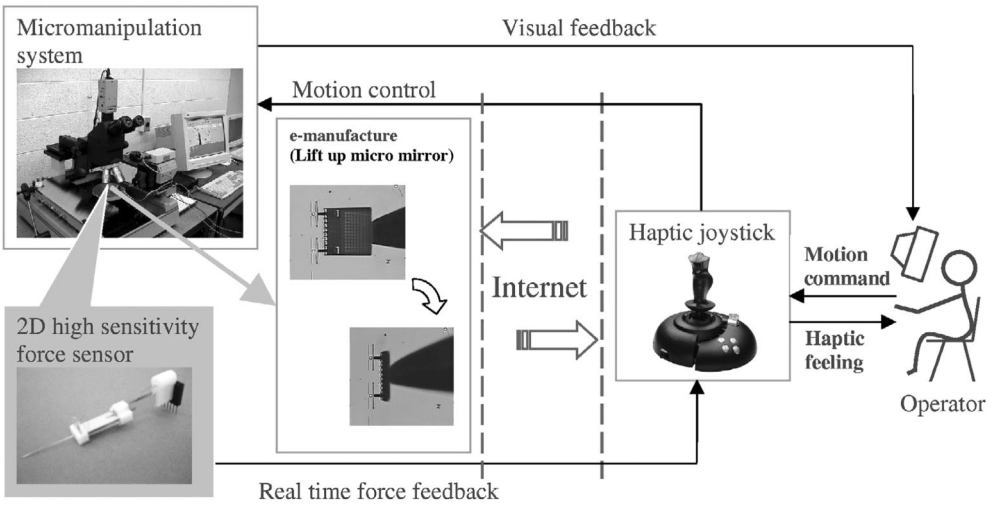

feedback. The joystick used in the system is a Microsoft SideWinder force feedback joystick.

The detailed procedures on the teleassembly of micromirror are as follows: before the lift-up, first, the operator drives the joystick to move the sensor tip to an initial position under the micromirror, then the tip is operated to move forward and upward simultaneously, as a result, the moving tip begins to lift the micromirror up until the mirror approaches an upright position. With the assistance of visual feedback from the microscope and camera system, and especially by force /haptic feedback, the task of remote microassembly via Internet is achieved reliably and easily.

Figure 10 shows a sketch of lifting up a micromirror by the sensor tip. From Figure 10, during the lift-up assembly, since the gravity force is not a dominative force in microenvironment, the forces exerted on the tip are mainly from the counteraction moments of the hinges and the latches, the friction forces due to the tip slide on the bottom surface of the mirror and the adhesion forces.

Figure 10 Sketch of lifting up a micromirror

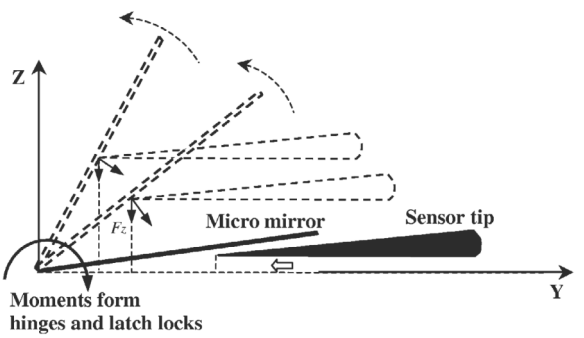

Figure 11 shows a successful remote assembly sequence of the micromirror using the developed micro E-manufacturing (remote assembly) system between Hong Kong and the USA via Internet.

In this experiment, by virtue of the visual feedback shown in Figure 11, the operator in the Center for Micro and Nano Systems at The Chinese University of Hong Kong can operate the joystick to remotely assemble the micromirror in the Robotic and Automation Lab at Michigan State University.

Moreover, during this teleoperation, the feedback of microcontact force also played an important role for this successful micro E-manufacturing. Figure 12 shows the recorded microforce in a period that is approximately corresponding from (i) to (vii) in the sequence of Figure 11. By feeding back this scaling microforce via Internet, the operator at the Hong Kong side had an apparent haptic/force feeling during the operation. This feeling had greatly enhanced the success rate of the teleassembly of micromirrors.

Although time delay of this experiment is about 1.5 s and the visual feedback is always slower than the force feedback; due to the use of event-synchronization method, the visual feedback was event-synchronized with the haptic/force feedback in this experiment. As a result, the operator at the Hong Kong side was sure that the video displayed was close in event to the force felt; this also improved the efficiency of tele-microassembly.

The experimental results on the teleassembly of micromirror demonstrated the performance of the developed Internet-based remote assembly (micro E-manufacturing) system.

Figure 11 The sequence of remotely assembling micromirror

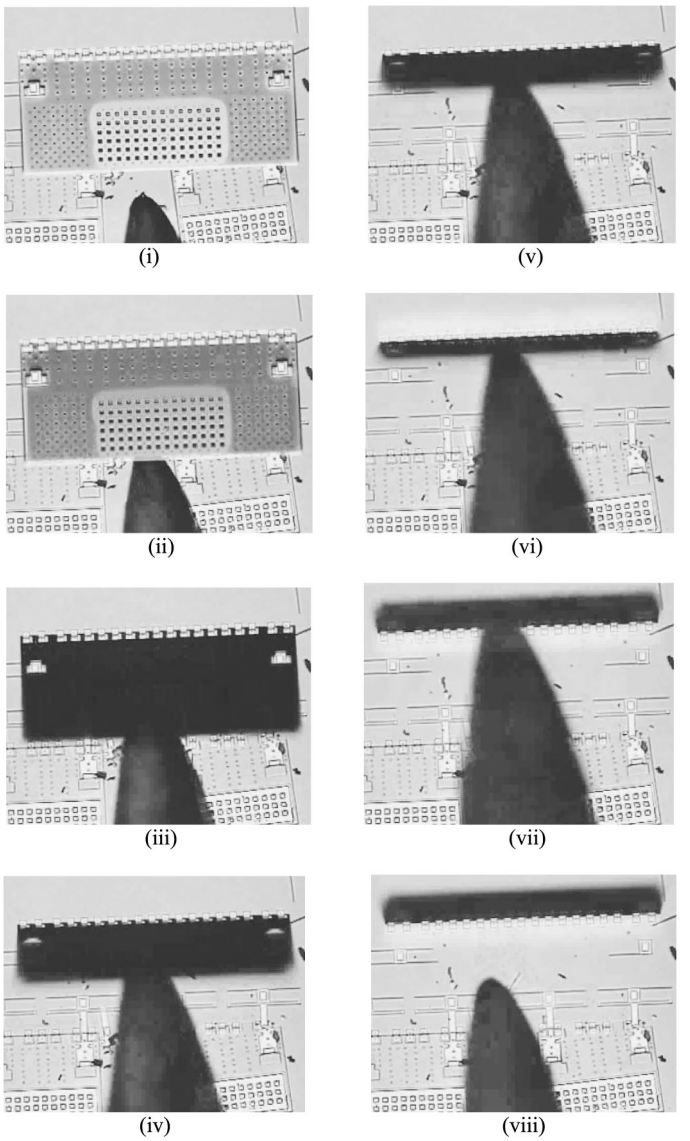

Figure 12 The detected microcontact force during teleassembly of the micromirror

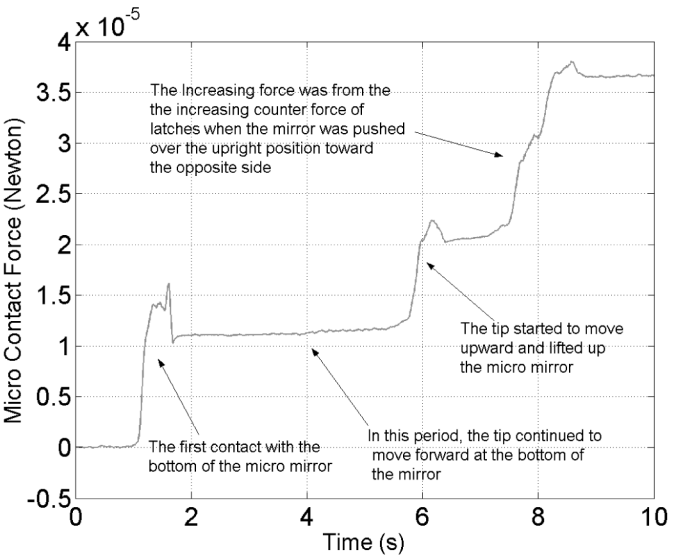

5. Conclusions

In this paper, PVDF film was used to fabricate high sensitivity force/force rate sensors for assembly and manufacture of microdevices such as surface MEMS structures fabricated using MUMPs process. Based on the developed sensory system, by integrating with a micromanipulator, the feedback of the microcontact force can greatly improve the reliability of micromanipulation. The technology was then extended to develop an Internet-based remote assembly (micro E-manufacturing) system for MEMS devices. Experimental results demonstrated the performance of the developed system. It will be a critical and major step towards the development of automated micromanufacturing processes for batch assembly of MEMS devices.

References

Benech, P., Chamberod, E. and Monllor, C. (1996), "Acceleration measurement using PVDF", *IEEE Transactions on Ultrasonics, Ferroelectrics, and Frequency Control*, Vol. 43 No. 5, pp. 838-43.

Böhringer, K.F., Fearing, R.S. and Goldberg, K.Y. (1999), "Microassembly", in Shimon Nof (Ed.), *The Handbook of Industrial Robotics*, 2nd ed., Wiley, New York, NY, pp. 1045-66.

Carrozza, M., Eisinberg, A., Menciassi, A., Campolo, D., Micera, S. and Dario, P. (2000), "Towards a force-controlled microgripper for assembling biomedical microdevices", *J. Micromech., Microeng*, Vol. 10, pp. 271-6.

Cohn, M.B., Böhringer, K.F., Novorolski, J.M., Singh, A., Keller, C.G., Goldberg, K.Y. and Howe, R.T. (1998), "Microassembly technologies for MEMS", *Proceedings of SPIE Conference on Micromachining and Microfabrication*, Invited paper/plenary session.

Fearing, R.S. (1995), "Survey of sticking effects for micro parts handling", *Proceedings of 1995 IEEE RSJ International Conference on Intelligent Robots and Systems*, pp. 212-17.

Fung, C.K.M., Elhajj, I., Li, W.J. and Xi, N. (2002), "A 2D PVDF force sensing system for micro-manipulation and micro-assembly", *Proceedings of the 2002 IEEE International Conference on Robotics and Automation*, pp. 1489-94.

IEEE Standard (1987), *An American National Standard: IEEE Standard on Piezoelectricity*, ANS/IEEE Std 176-1987.

Kenny, T. (2001), "Nanometer-scale force sensing with MEMS devices", *IEEE Sensors Journal*, Vol. 1 No. 2, pp. 148-57.

Koelemijer, S.K., Benmayor, C.L., Uehlinger, J-M. and Jacot, J. (1999), "Cost-effective micro-system assembly automation", *Proceedings of Emerging Technologies and Factory Automation*, Vol. 1, pp. 359-66.

Measurement Specialties Inc. (1999), "Piezo film sensors technical manual", *Internet Version.*

Nelson, B., Zhou, Y. and Vikramaditya, B. (1998), "Sensor-based micro-assembly of hybrid MEMS devices", *IEEE Control System Magazine*, Vol. 18, pp. 35-45.

Yamagata, Y. and Higuchi, T. (1995), "A micro-positioning device for precision automatic assembly using impact force of piezoelectric elements", *Proceedings of 1995 IEEE*

International Conference on Robotics and Automation, Vol. 3, pp. 666-71.

Zesch, W. and Fearing, R. (1998), "Alignment of microparts using force controlled pushing", SPIE Conference on Microrobotics and Micro-manipulation, 2-5 November, Boston, MA.

Further reading

Arai, F., Nonoda, Y., Fukuda, T. and Ooda, T. (1996), "New force measurement and micro grasping method using laser Raman spectrophotometer", *Proceedings of 1996 IEEE International Conference on Robotics and Automation*, pp. 2220-5.

Damjanovic, D., Muralt, P. and Setter, N. (2001), "Ferroelectric sensors", *IEEE Sensors Journal*, Vol. 1 No. 3, pp. 191-206.

Fatikow, S., Seyfried, J., Fahlbusch, S.T., Buerkle, A. and Schmoeckel, F. (2000), "A flexible microrobot-based microassembly station", *Journal of Intelligent and Robotic Systems*, Vol. 27, pp. 135-69.

Gehring, G.A., Cooke, M.D., Gregory, I.S., Karl, W.J. and Watts, R. (2000), "Cantilever unified theory and optimization for sensors and actuators", *Smart Material Structure*, Vol. 9, pp. 918-31.

Ikeda, T. (1990), *Fundamentals of Piezoelectricity*, Oxford University Press, Oxford.

Kimura, Y. and Yamagimachi, R. (1995), "Intracytoplasmic sperm injection in the mouse", *Biology of Reproduction*, Vol. 52 No. 4, pp. 709-20.

Lee, C., Itoh, T. and Suga, R. (1996), "Micromachined piezoelectric force sensors based on PZT thin films", *IEEE Transactions on Ultrasonics, Ferroelectrics, and Frequency Control*, Vol. 43 No. 4, pp. 553-9.

Roh, Y., Varadan, V.V. and Varadan, V.K. (2002), "Characterization of all the elastic, dielectric, and piezoelectric constants of uniaxially oriented poled PVDF films", *IEEE Transactions on Ultrasonics, Ferroelectrics, and Frequency Control*, Vol. 49 No. 6, pp. 836-46.

Weinberg, M.S. (1996), "Working equations for piezoelectric actuators and sensors", *IEEE Journal of Microelectromechanical Systems*, Vol. 8 No. 4, pp. 529-33.